A Novel Dynamic Model for Single-Dof Planar Mechanisms

Based on Instant Centers

Raffaele Di Gregorio

Department of Engineering, University of Ferrara

Via Saragat,1; 44122 FERRARA; Italy

T: +39-0532-974828, F: +39-0532-974870

E: raffaele.digregorio@unife.it

ABSTRACT

Many even complex machines employ single-dof planar mechanisms. The instantaneous kinematics of planar mechanisms can be fully understood by analyzing where the instant centers (ICs) of the relative motions among mechanism's links are located. ICs' positions depend only on the mechanism configuration in single-dof planar mechanisms and a number of algorithms that compute their location have been proposed in the literature. Once ICs positions are known, they can be exploited, for instance, to determine the velocity coefficients of the mechanism and the virtual work of the external forces applied to mechanism's links. Here, these and other ICs' properties are used to build a novel dynamic model and an algorithm that solves the dynamic problems of single-dof planar mechanisms. Then, the proposed model and algorithm are applied to a case study.

Keywords: planar mechanisms, instant centers, dynamics analysis, velocity coefficients.

1   INTRODUCTION

The vast literature (e.g., [1–6]) on single-degree-of-freedom (single-dof) planar mechanisms is motivated by the important role they play in many machines. The instantaneous (elementary) kinematics of planar mechanisms can be fully explained by analyzing the positions of the instant centers (ICs) of the relative motions among the mechanism links. In single-dof planar mechanisms, such positions depend only on the

mechanism configuration and a number of graphical and/or analytical techniques that determine them have been proposed [7–13] in the literature.

In short, a number of ICs (primary ICs) can be immediately found by inspection of the mechanism since they are ICs of relative motions between couples of links joined through a single-dof kinematic pair[1] [7]. Also, in general, the remaining ICs (secondary ICs) can be found by using the already located ICs and the Aronhold-Kennedy (A-K) theorem[2] with the aid of circle diagrams [7] or suitable tables [8]. Eventually, some mechanisms, named "indeterminate", exist where the A-K theorem is not sufficient to locate all the secondary ICs, and more cumbersome techniques have been proposed in the literature [8–11, 13] for locating all the ICs of these mechanisms.

The majority of the proposed techniques are graphical [7–11] for historical reasons and their automatic usage can be implemented through graphical software. Nevertheless, analytical techniques [12, 13] have been also proposed.

The availability of analytical techniques that compute ICs' coordinates in a reference fixed to the mechanism frame makes it possible to develop novel algorithms that analyze other aspects of mechanisms' behavior over their elementary kinematics. Actually, ICs allow computing the velocity coefficients (VCs) [1] of the mechanism and VCs enter both in statics and dynamics.

In particular, the dynamic model of a single-dof mechanism can be built with Eksergian's equation of motion [14, 15]. Such model directly relates the input generalized torque, applied by the actuator, to mechanism's generalized coordinate and its time derivatives (i.e., to the resulting motion of the mechanism) thus keeping only the pieces of information necessary to control the mechanism. This equation involves the VCs over the mass distribution data of the links and the active forces applied to them.

In this paper, a novel dynamic model for single-dof planar mechanisms is deduced, from Eksergian's equation, by systematically using the ICs positions to compute all the terms appearing in that equation. Then, an algorithm to solve the dynamic problems of single-dof planar mechanisms is presented which combines the novel dynamic model and the analytical technique this author previously proposed [13] for determining ICs' positions. Eventually, the algorithm is illustrated through a case study.

---

[1] Prismatic (P) or revolute (R) pairs and rolling (C_r) or slipping (C_s) contacts are the only kinematic pairs of planar mechanisms. P, R and C_r are single-dof pairs and uniquely determine the IC position of the relative motion between the joined links; whereas, the same IC is not uniquely located, but it must lie on the common normal at the contact point, for C_s, which is a two-dof pair [7].

[2] Let I_{rs} be the IC of the relative motion between any two links r and s, the A-K theorem states that "the instant center I_{ij} lies on the straight line through the instant centers I_{ki} and I_{kj} where link k may be any link different from links i and j" [7] (see Fig. 1a).

The paper is organized as follows. Section 2 briefly recalls some background concepts and the analytical technique proposed in [13]. Section 3 presents the dynamic model and the algorithms that solve the inverse and the direct dynamics problems. Then, Sec. 4 exemplifies the proposed algorithms through a case study, and Sec. 5 draws the conclusions.

2 BACKGROUND

The topology of any single-dof planar mechanism with m links, c_1 single-dof kinematic pairs, c_2 slipping contacts and n loops must adhere to the following formulas:

$$3m = 4 + 2\,c_1 + c_2 \tag{1a}$$
$$n = c_1 + c_2 - m + 1 \tag{1b}$$

which have been deduced from Chebychev-Grübler-Kutzbach formula and Euler's formula [1, 16], respectively. The linear elimination of m from Eqs. (1) yields

$$3n = c_1 + 2\,c_2 - 1 \tag{2}$$

The number, c_1, of single-dof kinematic pairs is equal to the number of primary ICs (i.e., the ICs whose positions are known by mechanism inspection); whereas, the number, c_2, of slipping contacts is equal to the number of ICs that lie on known straight lines. $(c_1 + 2\,c_2)$ is equal to the number of joint variables[3]. Moreover, let f be the number of scalar equations that can be written for each mechanism loop: f is equal to 3 if all the joint variables are introduced; whereas, it is equal to 2 if links' poses are assigned through oriented segments (i.e., complex numbers), embedded in the links, that are referred to a fixed frame[4] [1]. The latter approach, implemented through complex numbers, brings to write a closure equation system constituted of n complex equations which contain the generalized coordinate (input variable) q and 2n dependent (secondary) variables sufficient to directly determine the poses of all the links. Such system can be put into the following vector form:

---

[3] It is worth noting that, in single-dof planar mechanisms, the passive-joint variables are (c_1+2c_2-1) and the actuated-joint variable is one.

$$\mathbf{F}(q, \mathbf{p}) = \mathbf{0} \tag{3}$$

where $\mathbf{p}=(p_1, \ldots, p_{2n})^T$ is a 2n-tuple collecting all the secondary variables and $\mathbf{F} = (F_1, \ldots, F_{2n})^T$ is a 2n-tuple collecting all the scalar functions at the left-hand side of the 2n scalar closure equations.
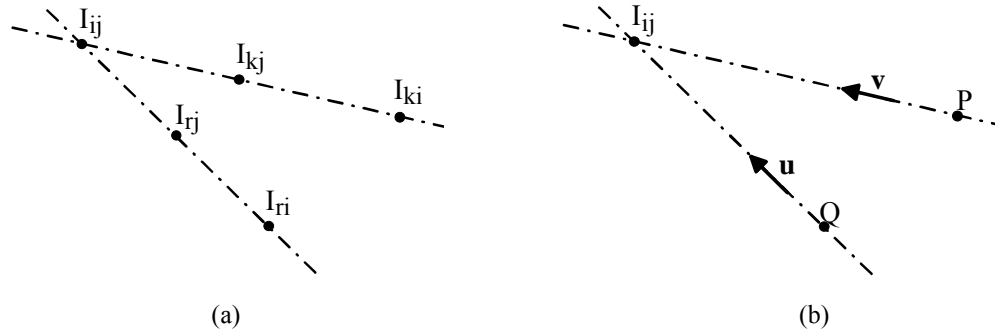

(a)   (b)

Figure 1: Intersection of two lines the instant center I_{ij} lies on: (a) the two lines are identified through the A-K theorem, (b) the two lines refer to either a slipping contact or a prismatic pair [13].

For an assigned value of q, the numerical or analytical solution of system (3) brings to determine the poses of all the mobile links through the computed values of the secondary variables. The knowledge of links' poses also provides the coordinates of all the primary ICs and the parametric equations of all the straight lines the secondary ICs lie on. These data are the input data of any graphical or analytical technique that determines the positions of all the secondary ICs [7–13].

The positions of the secondary ICs are sequentially computed one by one as common intersection of two lines, the sought-after IC lies on, in the mechanisms that are not "indeterminate" (i.e., in the majority of the possible cases) [13]. Since, according to the A-K theorem, the identification of the lines, the instant center I_{ij} lies on, relies on the already determined ICs, the first step of these techniques consists in the determination of the sequence, hereafter named S, to be used in this computation. This procedure is slightly modified in the indeterminate mechanisms [13], since a subset of ICs must be simultaneously (i.e., not sequentially) determined, but the determination of the sequence S still is the first step.

The sequence S depends only on the mechanism topology and must be computed only once. Therefore, the determination of the IC positions as a function of q (i.e., of the mechanism configuration) implements the following steps (see [13] for details): (i) the sequence S is determined from the mechanism topology; then, for

---

[4] In this case, differently from the use of joint variables, links' orientations are given through absolute angles that are independent

each value of q, (ii) system (3) is solved, and (iii) the positions of all the secondary ICs are sequentially computed by sequentially solving a number of linear systems of two equations in two unknowns.

Regarding step (iii), the two lines whose common intersection is the sought-after instant center, I_{ij} in Fig. 1, can be (a) lines passing through two known points (the instant centers I_{kj}, I_{ki}, I_{rj} and I_{ri} of Fig. 1a) or (b) lines passing through a known point (points P and Q of Fig.1b) with a given direction (the ones of the unit vectors **u** and **v** of Fig. 1b). In both cases, the following complex equation [13] can be written

$$w_1\, \mathbf{a} + w_2\, \mathbf{b} = \mathbf{c} \tag{4}$$

where **a**, **b** and **c** are known complex numbers representing known planar vectors; whereas, w_1 and w_2 are two scalar unknowns whose values locate I_{ij} on the two lines. For instance[5], $\mathbf{a}=(\mathbf{I}_{kj}–\mathbf{I}_{ki})$, $\mathbf{b}=(\mathbf{I}_{rj}–\mathbf{I}_{ri})$, $\mathbf{c}=(\mathbf{I}_{ri}–\mathbf{I}_{ki})$, $(\mathbf{I}_{ij}–\mathbf{I}_{ki})=w_1(\mathbf{I}_{kj}–\mathbf{I}_{ki})$ and $(\mathbf{I}_{ij}–\mathbf{I}_{ri})=–w_2(\mathbf{I}_{rj}–\mathbf{I}_{ri})$ in the case of Fig. 1a; also, $\mathbf{a}=\mathbf{u}$, $\mathbf{b}=\mathbf{v}$, $\mathbf{c}=(\mathbf{P}–\mathbf{Q})$, $(\mathbf{I}_{ij}–\mathbf{Q})=w_1\mathbf{u}$ and $(\mathbf{I}_{ij}–\mathbf{P})=–w_2\mathbf{v}$ in the case of Fig. 1b. The analytical solution of Eq. (4) can be straightforwardly written as follows[6]

$$w_1 = \frac{\text{Im}(\mathbf{c}\,\underline{\mathbf{b}})}{\text{Im}(\mathbf{a}\,\underline{\mathbf{b}})}, \qquad w_2 = \frac{\text{Im}(\mathbf{c}\,\underline{\mathbf{a}})}{\text{Im}(\mathbf{b}\,\underline{\mathbf{a}})} \tag{5}$$

The coordinates of the ICs can be used to compute the values of all the velocity ratios (velocity coefficients (VCs)) [1]. In particular, with the notation of Fig. 2, let $\dot{\theta}_{ji}$ and $\dot{s}_{ji}$ be the signed magnitudes of the relative angular velocity (in the case of instantaneous rotation) and of the relative translation velocity (in the case of instantaneous translation), respectively, between links j and i (Fig. 2), the following formulas hold

$$\frac{\dot{\theta}_{ji}}{\dot{\theta}_{ki}} = \frac{(\mathbf{I}_{kj} - \mathbf{I}_{ki}) \cdot (\mathbf{I}_{kj} - \mathbf{I}_{ji})}{\left\| \mathbf{I}_{kj} - \mathbf{I}_{ji} \right\|^2} \tag{6a}$$

$$\frac{\dot{s}_{ji}}{\dot{\theta}_{ki}} = -(\mathbf{I}_{kj} - \mathbf{I}_{ki}) \cdot \mathbf{u}_{ji} \tag{6b}$$

---

and the total number of introduced variables reduces itself to $(c_1+2c_2–n)$.

[5] In this definitions, all the vectors are represented through complex numbers.

[6] Hereafter, the underline denotes the complex conjugate; whereas, Re(·) and Im(·) denote the real and imaginary parts of (·), respectively.

$$\frac{\dot{s}_{ji}}{\dot{s}_{ri}} = \frac{(\mathbf{I}_{kj} - \mathbf{I}_{ki}) \cdot \mathbf{u}_{ji}}{(\mathbf{I}_{kr} - \mathbf{I}_{ki}) \cdot \mathbf{u}_{ri}} \tag{6c}$$

where the rotation angle θ_{ji} and θ_{ki} are positive if counterclockwise (Fig. 2a); whereas, the unit vector $\mathbf{u}_{ji}$ and $\mathbf{u}_{ri}$ are obtained from the unit vectors $\mathbf{t}_{ji}$ and $\mathbf{t}_{ri}$ (Fig. 2b), respectively, which give the positive directions of translation, through a counterclockwise rotation of 90°. Equation (6c) is simply obtained as the ratio of two different forms of Eq. (6b), one with $\dot{s}_{ji}$ and the other with $\dot{s}_{ri}$.

The dot products appearing in Eqs. (6) are all between collinear planar vectors (see the A-K theorem). Differently from VCs' usual expressions (i.e., ratios of two segments' lengths or one segment's length), those provided by Eqs. (6) give also the signs of the VCs.
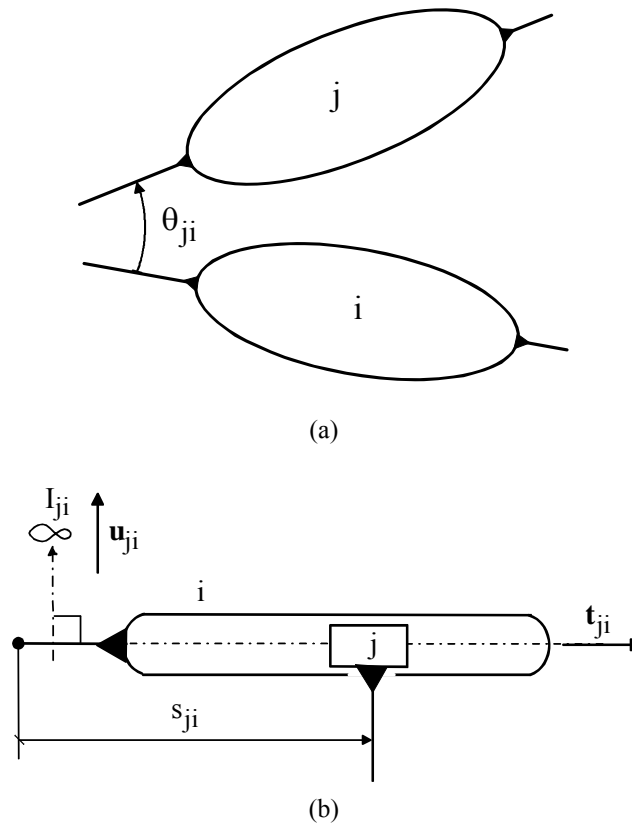

(a)

(b)

Figure 2: Instantaneous relative motion between links j and i: (a) instantaneous rotation (I_{ji} is a finite point of the motion plane; the motion is uniquely defined by I_{ji} and $\dot{\theta}_{ji}$), (b) instantaneous translation (I_{ji} is the point at infinity of the lines perpendicular to the translation direction; the motion is uniquely defined by the translation velocity $\dot{s}_{ji} \, t_{ji}$).

3 DYNAMIC MODEL

If only single-dof mechanisms with holonomic constraints not explicitly dependent on time are considered, their dynamic model can be deduced from Eksergian's equation [1, 15]:

$$Q = J\ddot{q} + \frac{1}{2}\frac{dJ}{dq}\dot{q}^2 \qquad (7)$$

where q is the generalized coordinate, Q is the generalized force collecting the contribution of all the active forces applied to mechanism's links, and J is the generalized inertia coefficient. J depends only on q and is related to the total kinetic energy, E, of the mechanism by the relationship

$$J = \frac{2E}{\dot{q}^2} \qquad (8)$$

In a single-dof planar mechanism with m links where link 1 is the frame (Fig. 3), let G_j, μ_j and λ_j be the center of mass, the mass and the inertia moment about its center of mass, respectively, of the j-th link, the explicit expressions of J and of its derivative with respect to q can be put in the form

$$J = \sum_{j=2,m} J_j v_j^2 \qquad (9a)$$

$$\frac{dJ}{dq} = \sum_{j=2,m}\left(\frac{dJ_j}{dq}v_j + 2J_j\frac{dv_j}{dq}\right)v_j \qquad (9b)$$

where the j-th term of the summations is related to the instantaneous motion of link j. In particular, if the instant center I_{j1} is a finite point of the motion plane[7],

$$J_j = \lambda_j + \mu_j(\mathbf{G}_j - \mathbf{I}_{j1})\cdot(\mathbf{G}_j - \mathbf{I}_{j1}) \qquad (10a)$$

$$\frac{dJ_j}{dq} = -2\mu_j(\mathbf{G}_j - \mathbf{I}_{j1})\cdot\frac{d\mathbf{I}_{j1}}{dq} \qquad (10b)$$

---

[7] It is worth reminding that, in this case, J_j is the inertia moment of link j about the instant center I_{j1} [1], which is related to λ_j by the Huygens-Steiner theorem, and that $(\mathbf{G}_j - \mathbf{I}_{j1})\cdot d\mathbf{G}_j = 0$.

$$v_j = \frac{\dot{\theta}_{j1}}{\dot{q}} \; ; \qquad\qquad\qquad (10c)$$

otherwise, that is, if the instant center I_{j1} is an ideal point located at infinity along the lines parallel to a unit vector $\mathbf{u}_{j1}$ (e.g., Fig. 2b with i=1),

$$J_j = \mu_j \qquad\qquad\qquad (11a)$$

$$\frac{dJ_j}{dq} = 0 \qquad\qquad\qquad (11b)$$

$$v_j = \frac{\dot{s}_{j1}}{\dot{q}} \qquad\qquad\qquad (11b)$$

The explicit expressions of the velocity coefficients, v_j, for j=2,…,m, must be chosen among Eqs. (6) by taking into account whether $\dot{q}$ is the signed magnitude of an angular velocity (e.g., $\dot{\theta}_{k1}$) or of a translation velocity (e.g., $\dot{s}_{r1}$). Relationships (6), (9) – (11) make it possible to compute J by using only the coordinates of a number of ICs and the mass distribution data of each link, since the coordinates of all the G_j, for j=2, …, m, can be easily computed as a function of q, together with the positions of the primary ICs, after the closure equation system (i.e., Eq. (3)) is solved.
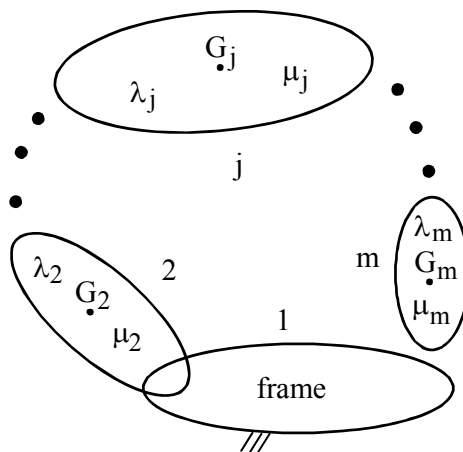

Figure 3: Generic scheme of a single-dof planar mechanism with m links (G_j, μ_j and λ_j, for j=2,…,m, are the center of mass, the mass and the inertia moment about its center of mass, respectively, of the j-th link).
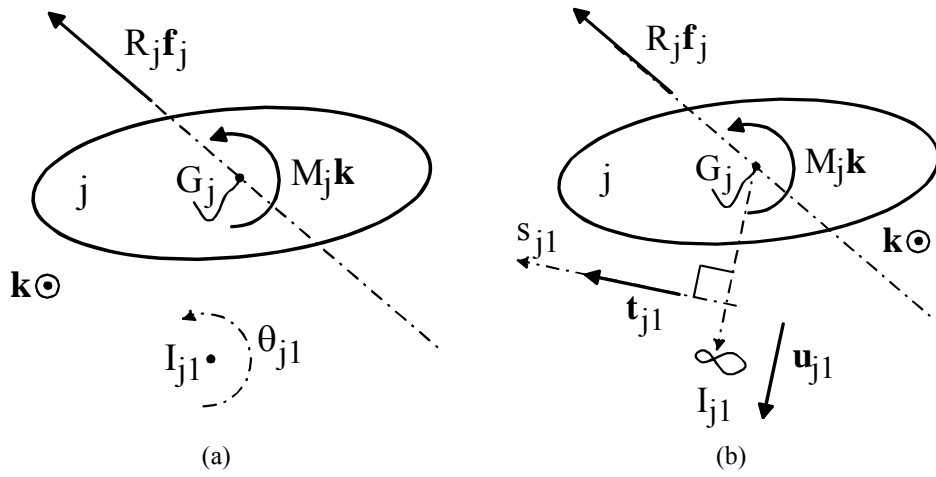
(a)   (b)

Figure 4: Link j loaded by the resultant torque, $M_j\mathbf{k}$, about G_j and the resultant force, $R_j\mathbf{f}_j$, of all the active forces applied to it: (a) the link performs an instantaneous rotation about I_{j1}, (b) the link performs an instantaneous translation parallel to $\mathbf{t}_{j1}$.

Regarding the generalized force Q, the following relationship holds

$$Q = \tau + \sum_{j=2,m} \alpha_j v_j \tag{12}$$

where τ is the generalized torque (usually applied by the actuator) that directly controls the generalized coordinate q; whereas, $\alpha_j v_j$ is the contribution to Q due to all the active forces applied to link j. Figure 4 shows link j loaded by the resultant torque, $M_j\mathbf{k}$, about G_j and the resultant force, $R_j\mathbf{f}_j$, of all the active forces applied to it[8]. With reference to Fig. 4, if the instant center I_{j1} is a finite point of the motion plane (Fig. 4a), then

$$\alpha_j = M_j + R_j\,[(\mathbf{G}_j - \mathbf{I}_{j1})\times\mathbf{f}_j]\cdot\mathbf{k} \tag{13a}$$

$$v_j = \frac{\dot{\theta}_{j1}}{\dot{q}}\,; \tag{13b}$$

---

[8] Here, M_j and R_j are the signed magnitudes of the two resultant, $\mathbf{k}$ is the unit vector normal to the motion plane that points toward the reader, and $\mathbf{f}_j$ is the unit vector that gives the positive direction for the resultant force.

otherwise, that is, if the instant center I_{j1} is an ideal point located at infinity along the lines parallel to a unit vector $\mathbf{u}_{j1}$ (Fig. 4b),

$$\alpha_j = R_j\,(\mathbf{f}_j \cdot \mathbf{t}_{j1}) \tag{14a}$$

$$\nu_j = \frac{\dot{s}_{j1}}{\dot{q}} \tag{14b}$$

Since active forces' data (i.e., M_j, R_j and $\mathbf{f}_j$ for j=2,…,m) are known, the explicit expression of Q is known after the VCs have been computed by using the ICs' positions and Eqs. (6).

The introduction of the above-deduced formulas into Eq. (7) yields

$$\tau + \sum_{j \in S_r} \{M_j + R_j[(\mathbf{G}_j - \mathbf{I}_{j1}) \times \mathbf{f}_j] \cdot \mathbf{k}\}\nu_j + \sum_{i \in S_t} R_i(\mathbf{f}_i \cdot \mathbf{t}_{i1})\,\nu_i = \ddot{q}\left[\sum_{j \in S_r}\left(\lambda_j + \mu_j\|\mathbf{G}_j - \mathbf{I}_{j1}\|^2\right)\nu_j^2 + \sum_{i \in S_t}\mu_i\nu_i^2\right] + $$
$$\dot{q}^2\left\{\sum_{i \in S_t}\mu_i\nu_i\frac{d\,\nu_i}{d\,q} + \sum_{j \in S_r}\left[\left(\lambda_j + \mu_j\|\mathbf{G}_j - \mathbf{I}_{j1}\|^2\right)\frac{d\,\nu_j}{d\,q} - \mu_j\nu_j(\mathbf{G}_j - \mathbf{I}_{j1})\cdot\frac{d\mathbf{I}_{j1}}{d\,q}\right]\nu_j\right\} \tag{15}$$

where S_r (S_t) is the subset of {2, …, m} that collects all the indices of the links that rotate (translate), with respect to the frame, and all the VCs are computed through Eqs. (6). Equation (15) is the sought-after dynamic model that contains, as input data, only the coordinates of the ICs, the mass distribution data and the data of the active forces.

The solution of the dynamics problems with the above-deduced formulas can be implemented by using the following two-stepped algorithm:

Step I (kinematics analysis)

- input data:

mechanism's topology and geometry, choice of the generalized coordinate q;

- procedure:

(I.a) the sequence S to follow for determining the ICs is computed by using mechanism's topology (see [13] for details);

(I.b) the continuous interval, q ranges in, is discretized to get a suitable set {q_1, …, q_r} of q values;

(I.c) for k=1,…,r,

    (I.c.1) Eq. (3) is solved with q=q_k and the corresponding values of the secondary variables, $\mathbf{p}_k$, is determined,

    (I.c.2) by using S, q_k and $\mathbf{p}_k$, the coordinates of all the necessary ICs are computed (see [13] for details),

    (I.c.3) by using the computed IC coordinates and Eqs. (6), the corresponding values of all the necessary VCs are computed;

(I.d) by using the computed discretized values of ICs' coordinates, the corresponding discretized values of their derivatives with respect to q are computed;

(I.e) by using the computed discretized values of the VCs, the corresponding discretized values of their derivatives with respect to q are computed;

Step II (dynamics analysis)

    - <u>input data:</u>

mass distribution data of the links (i.e., G_j, μ_j and λ_j for j=2,…,m), active forces' data, computed values of (q_k, $\mathbf{p}_k$) and of the corresponding ICs and VCs together with their derivatives with respect to q;

    - <u>procedure to solve the "Inverse Problem" (IP)[9]:</u>

(IP.a) the given q(t) is discretized to obtain a set of value (t_i, q_i),

(IP.b) the computed discretized values, (t_i, q_i), are used to numerically compute the discretized values, $(t_i, \dot{q}_i, \ddot{q}_i)$, of $\dot{q}(t)$ and of $\ddot{q}(t)$,

(IP.c) for each (t_i, q_i), the input data and the computed values $(t_i, \dot{q}_i, \ddot{q}_i)$ are introduced into Eq. (15) to straightforwardly compute the corresponding (t_i, τ_i);

    - <u>procedure to solve the "Direct Problem" (DP)[10]:</u>

(DP.a) the given $\tau(t)$ is discretized to obtain a set of values (t_i, τ_i),

(DP.b) the initial motion data, q(0) and $\dot{q}(0)$, the discretized values, (t_i, τ_i), of $\tau(t)$ and the input data are used to start an iterative numerical algorithm that integrates Eq. (15) [1], which is a non-linear differential equation in q(t), to compute the discretized values (t_i, q_i) of q(t).

---

[9] The IP is the determination of the generalized torque, $\tau(t)$, as a function of time, t, once the generalized coordinate, q(t), as a function of time is given.

3.1 Remarks

Step I involves only the topology and the geometry of the mechanism. Thus, if the mechanism geometry does not change (e.g., in mechanism analysis and/or control), it can be implemented only once and offline; then, the results can be used to solve many dynamics problems. For instance, the implementation of the above IP procedure can be repeatedly done online to plan and control the mechanism motion once Step-I results have been computed and stored.

Also, the number of ICs positions to compute (point (I.c.2) of Step I) depends on the necessary VCs. Since the VCs can be iteratively computed as follows

$$v_j = \frac{\dot{x}_{j1}}{\dot{q}} \equiv \frac{\dot{x}_{j1}}{\dot{x}_{(j-1)1}} \frac{\dot{x}_{(j-1)1}}{\dot{q}} \equiv \frac{\dot{x}_{j1}}{\dot{x}_{(j-1)1}} v_{j-1} , \tag{16}$$

where $\dot{x}_{j1}$ is equal to $\dot{\theta}_{j1}$, if link j rotates, or to $\dot{s}_{j1}$, if link j translates, the ICs necessary to compute all the VCs are the instant centers $I_{j(j-1)}$, for j=3,…,m, and I_{j1}, for j=2,…,m, (see Eqs. (6)), that is, only (2m–3) ICs[11]. Moreover, the unknowns w_1 and w_2 (see Eq. (4)) that must be computed to locate the ICs are always particular VCs [13]. For instance, the above-given definitions referred to the case of Fig. 1a, that is, $(I_{ij}–I_{ki})=w_1(I_{kj}–I_{ki})$ and $(I_{ij}–I_{ri})=–w_2(I_{rj}–I_{ri})$, bring to conclude (see also Eq. (6a)) that

$$w_1 = \frac{(I_{ij} - I_{ki}) \cdot (I_{kj} - I_{ki})}{\left\| I_{kj} - I_{ki} \right\|^2} \equiv \frac{\dot{\theta}_{kj}}{\dot{\theta}_{ij}} \tag{17a}$$

$$w_2 = - \frac{(I_{ij} - I_{ri}) \cdot (I_{rj} - I_{ri})}{\left\| I_{rj} - I_{ri} \right\|^2} \equiv - \frac{\dot{\theta}_{rj}}{\dot{\theta}_{ij}} \tag{17b}$$

Regarding points (I.d) and (I.e) of Step I, even though the existence of explicit expressions as a function of the generalized coordinate q cannot be guaranteed for IC coordinates, VCs and their derivatives in the general case, their numerical evaluation is often unnecessary. In general, the sequential use of explicit formulas should be always possible since IC coordinates and VCs can be computed by sequentially solving

---

[10] The DP is the determination of the generalized coordinate, q(t), as a function of time once the generalized torque, τ(t), as a function of time and the initial values, q(0) and $\dot{q}(0)$, are given.

linear systems of two equations in two unknowns whose solutions (see Eqs. (4) and (5)) are explicit expressions that can be analytically differentiated to give the explicit expressions of their derivatives. For instance, in the below-reported case study, all the IC coordinates, VCs and derivatives are computed by sequentially using explicit formulas. Also, these formulas have been simply introduced into a short MATHEMATICA [17] program to obtain the diagrams reported in Figs. 7 – 9 (i.e., no actual deduction of complete explicit formulas was necessary) without requiring special attention to numerical issues.

Step II requires the determination of the positions of the mass centers, G_j for j= 2,…,m, as a function of q. Such determination can be easily implemented. In fact, with reference to Fig. 5, let $\mathbf{z}_j$ and $\mathbf{g}_j$ be the complex numbers representing the planar vectors ($\mathbf{B}_j$–$\mathbf{A}_j$) and ($\mathbf{G}_j$–$\mathbf{A}_j$), both embedded in link j, they are related by the simple relationship

$$\mathbf{g}_j = \frac{\left\|\mathbf{G}_j - \mathbf{A}_j\right\|}{\left\|\mathbf{B}_j - \mathbf{A}_j\right\|} \mathbf{z}_j \, e^{\mathbf{i}\gamma_j} \qquad (18)$$

where the angle γ_j is constant (see Fig. 5) and $\mathbf{i} = \sqrt{-1}$. Likewise, the positions of other points fixed to link j can be determined as a function of q.
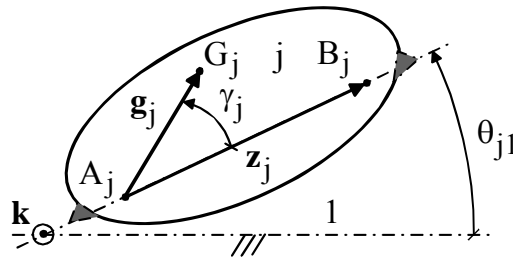

Figure 5: Link j: determination of G_j's position after the link pose, with respect to the frame, has been computed.

It is worth stressing that the choice of reducing link j's system of active forces to its center of mass, G_j (see Fig. 4 and Eqs. (13) – (15)), makes the computation burden lower, since the G_j positions are also necessary to compute the mass moment of inertia, J_j, about I_{j1} of the links that rotate (Eq. (10a)). Also, all the

---

[11] The total number of ICs is equal to the number of relative motions among the m links, that is, m(m–1)/2.

active forces whose lines of action are fixed with respect to link j can be reduced to G_j only once at the beginning of Step II.

The presented dynamic model is based on Eksergian's equation [15], which comes out of the 2nd-type Lagrangian formulation applied to single-dof mechanisms. As a consequence, it has the same advantages and drawbacks as this Lagrangian formulation when compared with the Newton-Euler formulation. Inside the same type of formulation, the computational efficiency of models and algorithms depends on the coordinates adopted to implement it [18]. The three most common types [18] of adopted coordinates are point coordinates, body coordinates, and joint coordinates (i.e., joint variables). According to [18], the most efficient ones are the body coordinates when cumbersome planar mechanisms that contain closed loops are considered. Whatever type of coordinates are adopted to build a dynamic model based on Eksergian's equation, they must be used to compute a number of VCs together with their derivatives. Three VCs for each mobile link (one related to link's angular velocity and the remaining two related to the two components of link's mass-center velocity (see chapter 12 of [1])), together with their derivatives, must be computed when body coordinates are used. On the contrary, only one VC for each mobile link, together with its derivative, is necessary when the proposed novel approach is used. Also, the proposed model uses parameters which are directly computed as functions of the generalized coordinate q; whereas, in the alternatives available in the literature [18], the determination of the VCs need the computation of point and angular velocities through suitable Jacobian matrices. The computation burden related to the determination of these Jacobians is in general heavier than the one involved in the computation of a few IC position vectors [1, 18].

4   CASE STUDY

This section illustrates how the above-presented model can be used to analyze the shaper mechanism[12] of Fig. 6 and to solve its inverse dynamics problem for a particular set of geometric and load data. Figure 6 shows the kinematic scheme of the shaper mechanism together with the adopted notations. With reference to Fig. 6, an Argand diagram, $(I_{21})xy$, fixed to link 1, the frame, with the instant center I_{21} as origin, has been introduced to represent planar vectors through complex numbers. The angle θ_{21} is the generalized coordinate, q; whereas, s_{34}, θ_{41}, θ_{51} and s_{61} are the secondary variables. The instant centers I_{21}, I_{32}, I_{34}, I_{41}, I_{54}, I_{65} and I_{61} are the primary ICs; whereas, I_{31} and I_{51} are the only secondary ICs necessary to build the model.
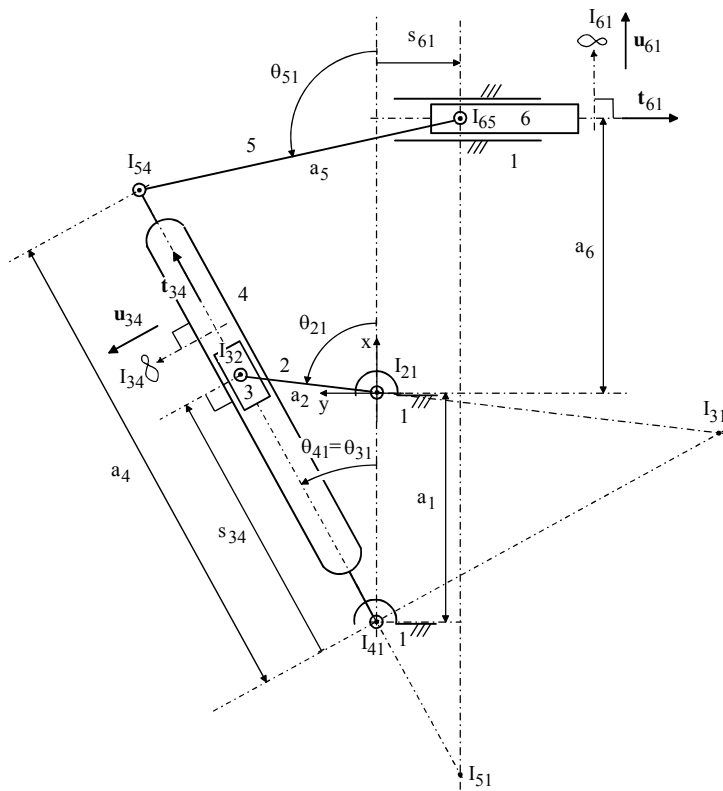
Figure 6: Shaper mechanism: kinematic scheme and notations.

With these notations, the following complex numbers $\mathbf{z}_j$ (see Fig. 5), for j= 1,…,6, can be associated to the links

---

[12] This linkage has been first proposed by James Nasmyth in 1836 [19]. Its topology is obtained from Watt-2 linkage's one by replacing two RRR dyads with as many RRP dyads.

$$\mathbf{z}_1 = -a_1, \ \mathbf{z}_2 = a_2 \ e^{i\theta_{21}}, \ \mathbf{z}_3 = s_{34} \ e^{i\theta_{41}}, \tag{19a}$$

$$\mathbf{z}_4 = a_4 \ e^{i\theta_{41}}, \ \mathbf{z}_5 = a_5 \ e^{i\theta_{51}}, \ \mathbf{z}_6 = a_6 - \mathbf{i} \ s_{61}, \tag{19b}$$

which make it possible to write the two loop equations

$$\mathbf{z}_1 + \mathbf{z}_3 = \mathbf{z}_2 \tag{20a}$$

$$\mathbf{z}_1 + \mathbf{z}_4 = \mathbf{z}_6 + \mathbf{z}_5 \tag{20b}$$

Equations (20) constitute the closure equation system (i.e., the system (3)) of the studied mechanism. This system yields the following formulas

$$s_{34} = \sqrt{(a_2 \cos\theta_{21} + a_1)^2 + a_2^2 \sin^2\theta_{21}} \tag{21a}$$

$$\theta_{41} = \sin^{-1}\left(\frac{a_2 \sin\theta_{21}}{s_{34}}\right) \tag{21b}$$

$$\theta_{51} = \cos^{-1}\left(\frac{a_4 \cos\theta_{41} - a_1 - a_6}{a_5}\right) \tag{21c}$$

$$s_{61} = a_5 \sin\theta_{51} - a_4 \sin\theta_{41} \tag{21d}$$

where the introduction of the bounds $\theta_{41} \in [-90°, 90°]$ and $\theta_{51} \in [0°, 180°]$ makes Eqs. (21b) and (21c) able to provide the unique correct value of θ_{41} and θ_{51}.

Equations (21a)–(21d) can be further rearranged to provide cumbersome explicit expressions of θ_{41}, θ_{51} and s_{61} as a function of θ_{21}. Nevertheless, from the numerical point of view, since each equation, over θ_{21}, contains only secondary variables that have been already computed through the previous equations, their direct sequential use is much more efficient.

The positions of the primary ICs can be given, by using complex numbers, as follows (see Fig. 6)

$$\mathbf{I}_{21} = 0; \ \ (\mathbf{I}_{41} - \mathbf{I}_{21}) = -a_1; \ \ \mathbf{t}_{34} = e^{i\theta_{41}}, \ \ \mathbf{u}_{34} = \mathbf{i} \, e^{i\theta_{41}}; \tag{22a}$$

$$(\mathbf{I}_{32} - \mathbf{I}_{21}) = a_2 \ e^{i\theta_{21}}; \ \ (\mathbf{I}_{54} - \mathbf{I}_{41}) = a_4 \ e^{i\theta_{41}}; \tag{22b}$$

$$(\mathbf{I}_{65}-\mathbf{I}_{54}) = -a_5\ e^{i\theta_{51}}\ ; \quad \mathbf{t}_{61} = -\mathbf{i}, \quad \mathbf{u}_{61} = 1; \tag{22c}$$

Moreover, the introduction of the relationships (see Fig. 6)

$$(\mathbf{I}_{32}-\mathbf{I}_{31}) = w_1(\mathbf{I}_{32}-\mathbf{I}_{21}), \quad (\mathbf{I}_{41}-\mathbf{I}_{31}) = w_2\ \mathbf{u}_{34} \tag{23a}$$

$$(\mathbf{I}_{54}-\mathbf{I}_{51}) = w_3(\mathbf{I}_{54}-\mathbf{I}_{41}), \quad (\mathbf{I}_{65}-\mathbf{I}_{51}) = w_4\ \mathbf{u}_{61}, \tag{23b}$$

where the scalar coefficients w_k, for $k=1,\dots,4$, are unknowns, makes it possible to write the following two vector equations in complex form

$$w_1(\mathbf{I}_{32}-\mathbf{I}_{21}) - w_2\ \mathbf{u}_{34} = (\mathbf{I}_{32}-\mathbf{I}_{21}) - (\mathbf{I}_{41}-\mathbf{I}_{21}) \equiv a_1 + a_2\ e^{i\theta_{21}} \tag{24a}$$

$$w_3(\mathbf{I}_{54}-\mathbf{I}_{41}) - w_4\ \mathbf{u}_{61} = (\mathbf{I}_{54}-\mathbf{I}_{65}) \equiv a_5\ e^{i\theta_{51}} \tag{24b}$$

Equations (24a) and (24b) are particular cases of Eq. (4) and can be immediately solved through formulas (5). So doing, the following analytic expressions of the unknowns are obtained

$$w_1 = \frac{\mathrm{Im}[-(a_1 + a_2\ e^{i\theta_{21}})\mathbf{i}e^{-i\theta_{41}}]}{\mathrm{Im}(-\mathbf{i}a_2\ e^{i\theta_{21}}e^{-i\theta_{41}})} \equiv 1 + \frac{a_1 \cos\theta_{41}}{a_2 \cos(\theta_{21}-\theta_{41})} \tag{25a}$$

$$w_2 = -\frac{\mathrm{Im}[(a_1 + a_2\ e^{i\theta_{21}})a_2\ e^{-i\theta_{21}}]}{\mathrm{Im}(\mathbf{i}a_2\ e^{-i\theta_{21}}e^{i\theta_{41}})} \equiv \frac{a_1 \sin\theta_{21}}{\cos(\theta_{21}-\theta_{41})} \tag{25b}$$

$$w_3 = \frac{\mathrm{Im}(a_5\ e^{i\theta_{51}})}{\mathrm{Im}(a_4\ e^{i\theta_{41}})} \equiv \frac{a_5 \sin\theta_{51}}{a_4 \sin\theta_{41}} \tag{25c}$$

$$w_4 = -\frac{\mathrm{Im}(a_5\ e^{i\theta_{51}}a_4\ e^{-i\theta_{41}})}{\mathrm{Im}(a_4\ e^{-i\theta_{41}})} \equiv \frac{a_5 \sin(\theta_{51}-\theta_{41})}{\sin\theta_{41}} \tag{25d}$$

Also, the coefficients w_k, $k=1,\dots,4$, coincide with the following VCs (see Eqs. (6) and (23)):

$$w_1 = \frac{(\mathbf{I}_{32}-\mathbf{I}_{31})\cdot(\mathbf{I}_{32}-\mathbf{I}_{21})}{\left\|\mathbf{I}_{32}-\mathbf{I}_{21}\right\|^2} \equiv \frac{\dot\theta_{21}}{\dot\theta_{31}} \equiv \frac{\dot\theta_{21}}{\dot\theta_{41}} \tag{26a}$$

$$w_2 = (\mathbf{I}_{41} - \mathbf{I}_{31}) \cdot \mathbf{u}_{34} \equiv -\frac{\dot{s}_{34}}{\dot{\theta}_{31}} \tag{26b}$$

$$w_3 = \frac{(\mathbf{I}_{54} - \mathbf{I}_{51}) \cdot (\mathbf{I}_{54} - \mathbf{I}_{41})}{\|\mathbf{I}_{54} - \mathbf{I}_{41}\|^2} \equiv \frac{\dot{\theta}_{41}}{\dot{\theta}_{51}} \tag{26c}$$

$$w_4 = (\mathbf{I}_{65} - \mathbf{I}_{51}) \cdot \mathbf{u}_{61} \equiv -\frac{\dot{s}_{61}}{\dot{\theta}_{51}} \tag{26d}$$

Equations (16) and (26) allow the computation of the explicit expressions of the velocity coefficients v_j, $j=2,\dots,6$, by using expressions (25) as follows

$$v_2 = 1; \quad v_3 \equiv v_4 = \frac{1}{w_1}; \quad v_5 = \frac{1}{w_3 w_1}; \quad v_6 = -\frac{w_4}{w_3 w_1} \tag{27}.$$

Since, now, all the explicit expressions of the necessary IC positions and VCs are available, their derivatives with respect to θ_{21} (i.e., to q) that appear in Eq. (15) can be computed as follows[13]

$$\frac{dv_2}{d\theta_{21}} = 0 \tag{28a}$$

$$\frac{dv_3}{d\theta_{21}} = \frac{dv_4}{d\theta_{21}} = -\frac{1}{w_1^2}\left(\frac{dw_1}{d\theta_{21}}\right) \equiv -\frac{1}{w_1^2}\left(\frac{\partial w_1}{\partial \theta_{41}}v_4 + \frac{\partial w_1}{\partial \theta_{21}}\right) \tag{28b}$$

$$\frac{dv_5}{d\theta_{21}} = \frac{1}{w_3}\frac{dv_4}{d\theta_{21}} - \frac{v_4}{w_3^2}\left(\frac{dw_3}{d\theta_{21}}\right) \equiv \frac{1}{w_3}\frac{dv_4}{d\theta_{21}} - \frac{v_4}{w_3^2}\left(\frac{\partial w_3}{\partial \theta_{41}}v_4 + \frac{\partial w_3}{\partial \theta_{51}}v_5\right) \tag{28c}$$

$$\frac{dv_6}{d\theta_{21}} = -w_4\frac{dv_5}{d\theta_{21}} - v_5\frac{dw_4}{d\theta_{21}} \equiv -w_4\frac{dv_5}{d\theta_{21}} - v_5\left(\frac{\partial w_4}{\partial \theta_{41}}v_4 + \frac{\partial w_4}{\partial \theta_{51}}v_5\right) \tag{28d}$$

and (see Eqs. (22) and (23))

---

[13] It is worth reminding that $\dfrac{dx}{dq} = \dfrac{\dot{x}}{\dot{q}}$ in single-dof mechanisms with holonomic constraints not explicitly dependent on time [1].

$$\frac{d\mathbf{I}_{21}}{d\theta_{21}} = \frac{d\mathbf{I}_{41}}{d\theta_{21}} = 0 \tag{29a}$$

$$\frac{d\mathbf{I}_{31}}{d\theta_{21}} = -\frac{dw_2}{d\theta_{21}}\mathbf{u}_{34} - w_2 \frac{d\mathbf{u}_{34}}{d\theta_{21}} = \left[w_2 v_4 - \left(\frac{\partial w_2}{\partial\theta_{21}} + v_4 \frac{\partial w_2}{\partial\theta_{41}} \right)\mathbf{i} \right] e^{i\theta_{41}} \tag{29b}$$

$$\frac{d\mathbf{I}_{51}}{d\theta_{21}} = \frac{d\mathbf{I}_{65}}{d\theta_{21}} - \frac{dw_4}{d\theta_{21}}\mathbf{u}_{61} = -\mathbf{i}\,v_6 - v_5 \frac{\partial w_4}{\partial\theta_{51}} - v_4 \frac{\partial w_4}{\partial\theta_{41}} \tag{29c}$$

where

$$\frac{\partial w_1}{\partial\theta_{21}} = \frac{a_1 \cos\theta_{41} \sin(\theta_{21} - \theta_{41})}{a_2 \cos^2(\theta_{21} - \theta_{41})}; \qquad \frac{\partial w_1}{\partial\theta_{41}} = -\frac{a_1 \sin\theta_{21}}{a_2 \cos^2(\theta_{21} - \theta_{41})}; \tag{30a}$$

$$\frac{\partial w_2}{\partial\theta_{21}} = \frac{a_1 \cos\theta_{41}}{\cos^2(\theta_{21} - \theta_{41})}; \qquad \frac{\partial w_2}{\partial\theta_{41}} = \frac{a_1 \sin\theta_{21} \sin(\theta_{21} - \theta_{41})}{\cos^2(\theta_{21} - \theta_{41})}; \tag{30b}$$

$$\frac{\partial w_3}{\partial\theta_{41}} = -\frac{a_5 \sin\theta_{51} \cos\theta_{41}}{a_4 \sin^2\theta_{41}}; \qquad \frac{\partial w_3}{\partial\theta_{51}} = \frac{a_5 \cos\theta_{51}}{a_4 \sin\theta_{41}}; \tag{30c}$$

$$\frac{\partial w_4}{\partial\theta_{41}} = -\frac{a_5 \sin\theta_{51}}{\sin^2\theta_{41}}; \qquad \frac{\partial w_4}{\partial\theta_{51}} = \frac{a_5 \cos(\theta_{51} - \theta_{41})}{\sin\theta_{41}}; \tag{30d}$$

Formulas (21), (22), (25), (27)–(29) are all the explicit expressions necessary to implement Step I for the shaper mechanism of Fig. 6. In this case, Step I can be simply implemented by sequentially using these formulas since each formula contains only terms that have been already computed through the previous formulas. Figures 7 shows the velocity coefficients v_3, v_5 and v_6 as a function of θ_{21} for the shaper mechanism with the following geometry: a_1=0.2m, a_2=0.1m, a_4=0.4m, a_5=0.2m, a_6=0.2m.

Eventually, the dynamic model of the shaper mechanism is (see Eq. (15))

$$\tau + R_6 v_6 \operatorname{Re}\left(\underline{\mathbf{f}}_6 \mathbf{t}_{61}\right) + \sum_{j=2,5}\left\{ M_j + R_j \operatorname{Im}\left[(\mathbf{G}_j - \mathbf{I}_{j1})\mathbf{f}_j \right] \right\} v_j = \ddot{\theta}_{21}\left[\mu_6 v_6^2 + \sum_{j=2,5}\left(\lambda_j + \mu_j \|\mathbf{G}_j - \mathbf{I}_{j1}\|^2 \right) v_j^2 \right] +$$

$$\dot{\theta}_{21}^2\left\{ \mu_6 v_6 \frac{dv_6}{d\theta_{21}} - \mu_3 v_3^2 \operatorname{Re}\left[(\mathbf{G}_3 - \mathbf{I}_{31}) \frac{d\mathbf{I}_{31}}{d\theta_{21}} \right] - \mu_5 v_5^2 \operatorname{Re}\left[(\mathbf{G}_5 - \mathbf{I}_{51}) \frac{d\mathbf{I}_{51}}{d\theta_{21}} \right] + \sum_{j=2,5}\left(\lambda_j + \mu_j \|\mathbf{G}_j - \mathbf{I}_{j1}\|^2 \right) \frac{d v_j}{d\theta_{21}} v_j \right\} \tag{31}$$

where all the explicit expressions of ICs' position vectors, of the VCs and of their derivatives are given by formulas (21), (22), (25), (27)–(29); also, all the planar vectors are expressed through the associated complex numbers, and the following relationship between any two planar vectors, $\boldsymbol{a}$ and $\boldsymbol{b}$, and the associated complex numbers, $\mathbf{a}$ and $\mathbf{b}$, has been used

$$\underline{\mathbf{a}}\mathbf{b} = \boldsymbol{a}\cdot\boldsymbol{b} + \mathbf{i}[(\boldsymbol{a}\times\boldsymbol{b})\cdot\mathbf{k}] \tag{32}$$

By using the mass distribution data of Table 1 and the same mechanism geometry as Fig. 7, Fig. 8 shows the generalized inertia coefficient, J, of the mechanism and its derivative with respect to θ_{21} as a function of θ_{21}. Also, Fig. 9 shows the generalized torque, τ, (applied by an actuator which directly controls the joint variable θ_{21}) as a function of θ_{21}, computed through Eq. (31), in the case that $\dot{\theta}_{21} = 20\,\mathrm{rpm}$, $\ddot{\theta}_{21} = 0$ and that the only active forces applied to mechanism are links' weights and a cutting force of 500 N with direction $\mathbf{t}_{61}$, applied to link 6 during its active stroke.

Table 1: Mass distribution data of shaper mechanism' s links (Fig. 6): j is the link number, μ_j is the mass of link j in [kg] and λ_j is link-j's mass moment of inertia, in [kg m²], about its mass center, G_j, that is assigned according to Fig. 5 and Eqs. (18) and (19).

Link No.	G_j	μ_j [kg]	λ_j [kg m²]
2	$G_2 \equiv I_{21}$	4.90088	0.0245044
3	$G_3 \equiv I_{32}$	0.196035	0.00196035
4	$(\mathbf{G}_4 - \mathbf{I}_{41}) = 0.5\,\mathbf{z}_4$	7.488	0.09984
5	$(\mathbf{G}_5 - \mathbf{I}_{65}) = 0.5\,\mathbf{z}_5$	2.496	0.00832
6	$G_6 \equiv I_{65}$	9.75	–

5 CONCLUSIONS

A novel dynamic model for single-dof planar mechanisms has been presented. The proposed model systematically uses the coordinates of a number of instant centers, thus making visible the relationship between kinematics and dynamics of the mechanism. This feature is appealing during both the analysis and the synthesis of any mechanism.

Based on the proposed model and on the analytical techniques that determine the coordinates of all the instant centers during the mechanism motion, a two-stepped algorithm has been proposed to sequentially solve first the kinematics analyses necessary to provide the input data of the model and, then, the dynamics problems with the novel model.

In order to better illustrate how the proposed notations and algorithms are applied to a real case, the dynamic model of a shaper mechanism has been built and its inverse dynamics problem has been solved for a given set of data. This case study has highlighted that the proposed model and algorithms are simple to use and numerically effective.

As far as this author is aware, even though some basic concepts the proposed model is based on are known in the literature, this is the first time that they are fully exploited to provide an analytic relationship between ICs' positions and the dynamic behavior of the mechanism.
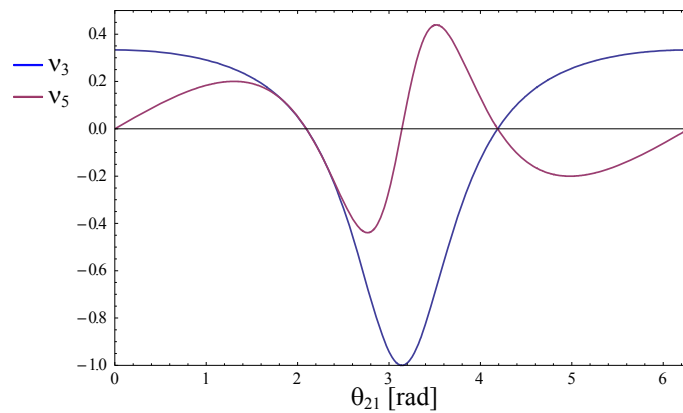
(a)
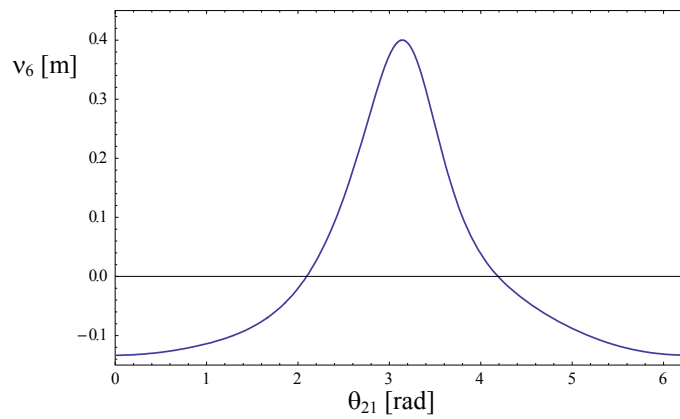
(b)

Figure 7: Velocity coefficients as a function of θ_{21} (a_1=0.2m, a_2=0.1m, a_4=0.4m, a_5=0.2m, a_6=0.2m): (a) v_3 and v_5, (b) v_6.

(a)

(b)

Figure 8: The generalized inertia coefficient, J, (a) and its derivative with respect to θ_{21} (b) of the shaper mechanism with the geometry of Fig. 7 and the mass distribution data of Table 1 as a function of θ_{21}.

Figure 9: Generalized inertia torque, τ, as a function of θ_{21} in the case $\dot{\theta}_{21} = 20$ rpm, $\ddot{\theta}_{21} = 0$ and a cutting force of 500 N.

REFERENCES

[1] Paul, B., 1979, "Kinematics and dynamics of planar machinery," Prentice-Hall, Inc., Englewood Cliffs, New Jersey (USA).

[2] Gans, R.F., 1991, "Analytical kinematics: analysis and synthesis of planar mechanisms," Butterworth-Heinemann Inc., Boston, Massachusetts (USA).

[3] Butcher, E.A., and Hartman, C., 2005, "Efficient enumeration and hierarchical classification of planar simple-jointed kinematic chains: Application to 12- and 14-bar single degree-of-freedom chains," Mechanism and Machine Theory, Vol. 40, No. 9 (September, 2005), pp. 1030-1050.

[4] Cardona, A., and Pucheta, M., 2007, "An automated method for type synthesis of planar linkages based on a constrained subgraph isomorphism detection," Multibody System Dynamics, Vol. 18, No. 2, pp. 233-258.

[5] Murray, A.P., Schmiedeler, J.P., and Korte, B.M., 2008, "Kinematic Synthesis of Planar, Shape-Changing Rigid-Body Mechanisms," ASME J. of Mechanical Design, Vol. 130, No. 3, pp. 032302-(*10 pages*).

[6] Kong, X., and Huang, C., 2009, "Type synthesis of single-DOF single-loop mechanisms with two operation modes," Procs. of ASME/IFToMM International Conference on Reconfigurable Mechanisms and Robots, ReMAR 2009, June 22-24, 2009, London (UK), pp. 136-141.

[7] Barton, L. O., 1993, "Mechanism Analysis: simplified graphical and analytical techniques," 2nd Ed., Marcel Dekker, Inc., New York (USA).

[8] Klein, A.W., 1917, "Kinematics of Machinery," McGraw-Hill Book Company, Inc., New York.

[9] Foster, D.E., and Pennock, G.R., 2003, "A graphical method to find the secondary instaneous centers of zero velocity for the double butterfly linkage," ASME J. of Mechanical Design, 125(2): 268-274.

[10] Pennock, G.R., and Kinzel E.C., 2004, "Path curvature of the single flier eight-bar linkage," ASME J. of Mechanical Design, 126(3): 470-477.

[11] Foster, D.E., and Pennock, G.R., 2005, "Graphical methods to locate the secondary instantaneous centers of single-degree-of-freedom indeterminate linkages," ASME J. of Mechanical Design, 127(2): 249-256.

[12] Yan, H.-S., and Hsu, M.-H., 1992, "An analytical method for locating instantaneous velocity centers," In Proc. of the 22nd ASME Biennial Mechanisms Conference, DE-Vol. 47, pp. 353-359, Scottsdale, AZ (USA), September 13-16, 1992.

[13] Di Gregorio, R., 2008, "An Algorithm for Analytically Calculating the Positions of the Secondary Instant Centers of Indeterminate Linkages," ASME J. of Mechanical Design, 130(4): 042303-(1:9).

[14] Wittenbauer, F., 1923, "Graphische Dynamik," Springer-Verlag, Berlin.

[15] Eksergian, R., 1928, "Dynamical analysis of machines," Ph.D. Dissertation, Clark University [15 articles published on J. of the Franklin Institute, Voll. 209–211 (1930–1931), report an extended version of this thesis]

[16] Angeles, J., 1988, "Rational Kinematics," Springer-Verlag, Inc., New York (USA).

[17] Wolfram, S., 2003, " The MATHEMATICA book, 5th Edition", Wolfram Media, Witney (UK).

[18] Nikravesh, P. E., 2007, "Planar multibody dynamics: formulation, programming, and applications," CRC Press, Boca Raton, FL (USA).

[19] Roe, J. W., 1926, "English and American tool builders," McGraw-Hill, Inc., New York (USA).

List of Table Captions

Table 1: Mass distribution data of shaper mechanism' s links (Fig. 6): j is the link number, μ_j is the mass of link j in [kg] and λ_j is link-j's mass moment of inertia, in [kg m^2], about its mass center, G_j, that is assigned according to Fig. 5 and Eqs. (18) and (19).
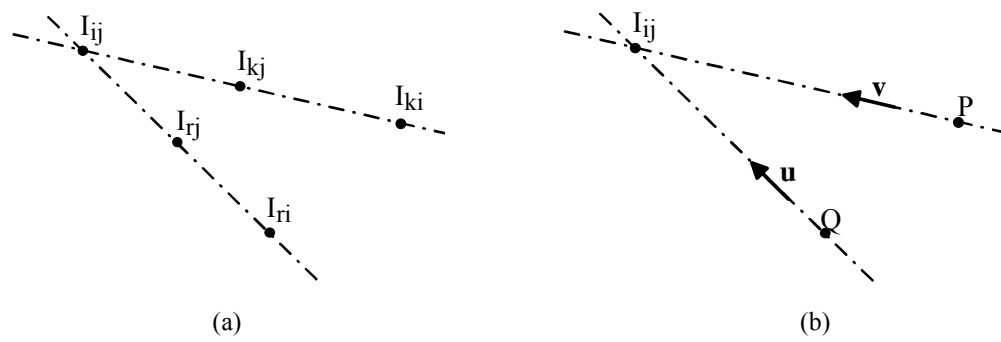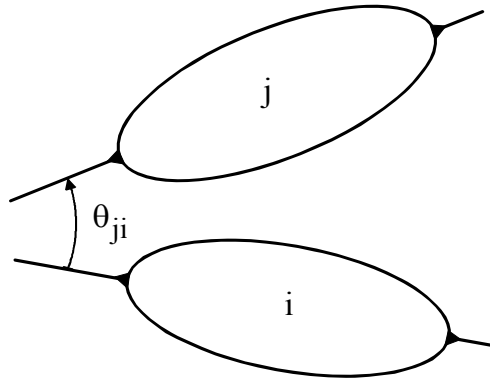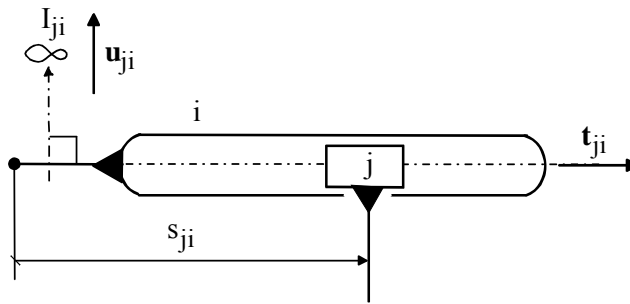
List of Figure Captions

Figure 1: Intersection of two lines the instant center I_{ij} lies on: (a) the two lines are identified through the A-K theorem, (b) the two lines refer to either a slipping contact or a prismatic pair [13].

Figure 2: Instantaneous relative motion between links j and i: (a) instantaneous rotation (I_{ji} is a finite point of the motion plane; the motion is uniquely defined by I_{ji} and $\dot{\theta}_{ji}$), (b) instantaneous translation (I_{ji} is the point at infinity of the lines perpendicular to the translation direction; the motion is uniquely defined by the translation velocity $\dot{s}_{ji}\, t_{ji}$).
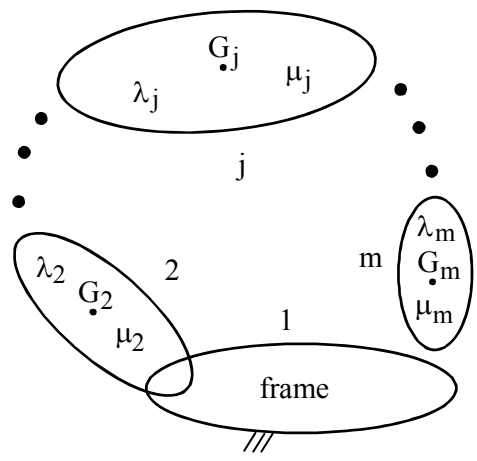
Figure 3: Generic scheme of a single-dof planar mechanism with m links (G_j, μ_j and λ_j, for j=2,…,m, are the center of mass, the mass and the inertia moment about its center of mass, respectively, of the j-th link).

Figure 4: Link j loaded by the resultant torque, $M_j\mathbf{k}$, about G_j and the resultant force, $R_j\mathbf{f}_j$, of all the active forces applied to it: (a) the link performs an instantaneous rotation about I_{j1}, (b) the link performs an instantaneous translation parallel to $\mathbf{t}_{j1}$.

Figure 5: Link j: determination of G_j's position after the link pose, with respect to the frame, has been computed.

Figure 6: Shaper mechanism: kinematic scheme and notations.

Figure 7: Velocity coefficients as a function of θ_{21} (a_1=0.2m, a_2=0.1m, a_4=0.4m, a_5=0.2m, a_6=0.2m): (a) v_3 and v_5, (b) v_6.

Figure 8: The generalized inertia coefficient, J, (a) and its derivative with respect to θ_{21} (b) of the shaper mechanism with the geometry of Fig. 7 and the mass distribution data of Table 1 as a function of θ_{21}.

Figure 9: Generalized inertia torque, τ, as a function of θ_{21} in the case $\dot{\theta}_{21} = 20$ rpm, $\ddot{\theta}_{21} = 0$ and a cutting force of 500 N.

Table 1: Mass distribution data of shaper mechanism' s links (Fig. 6): j is the link number, μ_j is the mass of link j in [kg] and λ_j is link-j's mass moment of inertia, in [kg m^2], about its mass center, G_j, that is assigned according to Fig. 5 and Eqs. (18) and (19).

Link No.	G_j	μ_j [kg]	λ_j [kg m^2]
2	$G_2 \equiv I_{21}$	4.90088	0.0245044
3	$G_3 \equiv I_{32}$	0.196035	0.00196035
4	$(\mathbf{G}_4 - \mathbf{I}_{41}) = 0.5\, \mathbf{z}_4$	7.488	0.09984
5	$(\mathbf{G}_5 - \mathbf{I}_{65}) = 0.5\, \mathbf{z}_5$	2.496	0.00832
6	$G_6 \equiv I_{65}$	9.75	–

Figure 1: Intersection of two lines the instant center I_{ij} lies on: (a) the two lines are identified through the A-K theorem, (b) the two lines refer to either a slipping contact or a prismatic pair [13].

(a)

(b)

Figure 2: Instantaneous relative motion between links j and i: (a) instantaneous rotation (I_{ji} is a finite point of the motion plane; the motion is uniquely defined by I_{ji} and $\dot{\theta}_{ji}$), (b) instantaneous translation (I_{ji} is the point at infinity of the lines perpendicular to the translation direction; the motion is uniquely defined by the translation velocity $\dot{s}_{ji}\, t_{ji}$).

Figure 3: Generic scheme of a single-dof planar mechanism with m links (G_j, μ_j and λ_j, for j=2,…,m, are the center of mass, the mass and the inertia moment about its center of mass, respectively, of the j-th link).

Figure 4: Link j loaded by the resultant torque, $M_j\mathbf{k}$, about G_j and the resultant force, $R_j\mathbf{f}_j$, of all the active forces applied to it: (a) the link performs an instantaneous rotation about I_{j1}, (b) the link performs an instantaneous translation parallel to $\mathbf{t}_{j1}$.

Figure 5: Link j: determination of G_j's position after the link pose, with respect to the frame, has been computed.
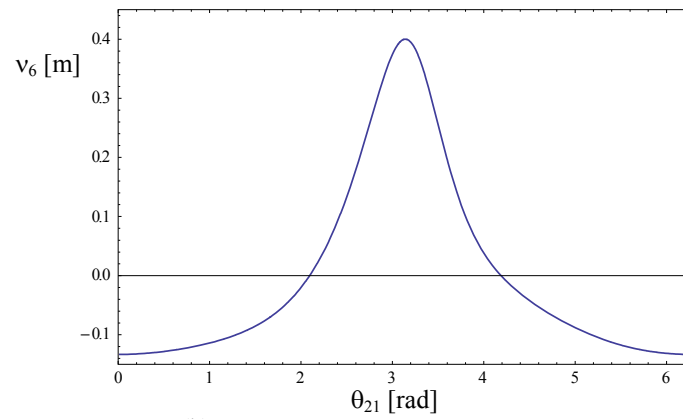
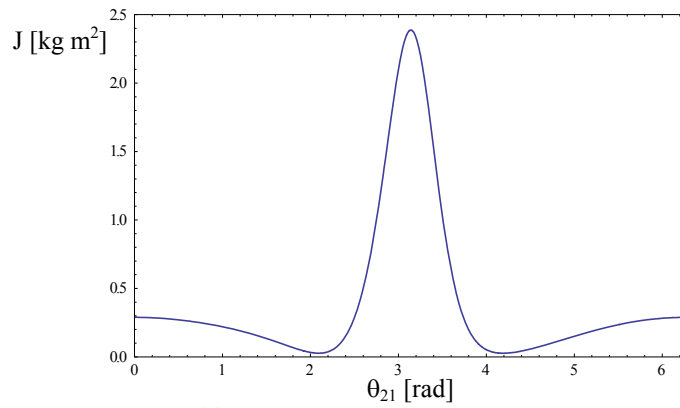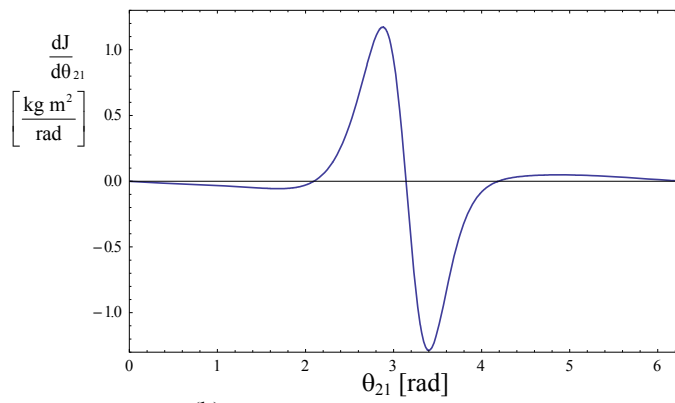**Figure 6:** Shaper mechanism: kinematic scheme and notations.

(a)

(b)

Figure 7: Velocity coefficients as a function of θ_{21} (a_1=0.2m, a_2=0.1m, a_4=0.4m, a_5=0.2m, a_6=0.2m): (a) ν_3 and ν_5, (b) ν_6.

Figure 8: The generalized inertia coefficient, J, (a) and its derivative with respect to θ_{21} (b) of the shaper mechanism with the geometry of Fig. 7 and the mass distribution data of Table 1 as a function of θ_{21}.
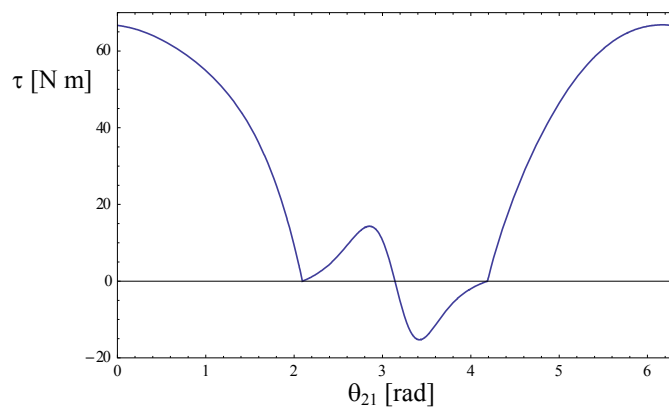
Figure 9: Generalized inertia torque, τ, as a function of θ_{21} in the case $\dot{\theta}_{21} = 20$ rpm, $\ddot{\theta}_{21} = 0$ and a cutting force of 500 N.